

Quantum Chemical Calculations on Vibrational and Electronic Structure Of 3-(4-Methoxybenzoyl) Propionic Acid

T.Chithambarathanu^{1*}, K.Vanaja², J.Daisymagdaline²

^{1*}Department Of Physics, S.T.Hindu College, Nagercoil, India

²Department Of Physics, Rani Anna Government Arts College For Women, Tirunelveli, India

Corresponding author: T.Chithambarathanu

Abstract : The Vibrational Spectral Analysis Was Carried Out By Using FT-IR And FT-Raman Spectroscopy In The Range 450 – 4000cm⁻¹ and 50 – 4000cm⁻¹ Respectively For 3 – (4 – Methoxybenzoyl) Propionic Acid (C₉H₁₀O₃) Molecule. The Molecular Structure, Fundamental Vibrational Frequencies And Intensity Of The Vibrational Bands Were Interpreted With The Aid Of Structure Optimizations And Normal Coordinate Force Field Calculations Based HF And DFT With B3LYP/6-311++G(D,P) And B3LYP/6-31++G(D,P) Basis Sets. The Complete Vibrational Assignments Of Wavenumbers Were Made On The Basis Of Potential Energy Distribution (PED). The Calculated HOMO And LUMO Energies Show That Charge Transfer Occurs Within The Molecule. The Reactivity Sites Were Identified By Mapping The Electron Density Into Electrostatic Potential Surface (MESP). The Stability Of The Molecule Arising From Hyper Conjugative Interactions And Charge Delocalization Has Been Analysed Using Natural Bond Analysis (NBO). The UV-Vis Absorption Spectra Of The Compound Were Recorded In The Range Of 200 – 400 Nm In Water And Ethanol Solvents.

Keywords: 3 - (4 - Methoxybenzoyl) Propionic Acid, DFT, HOMO, LUMO, NBO

Date of Submission: 12-03-2018

Date of acceptance: 26-03-2018

I. INTRODUCTION

The Propionic Acid Inhibits The Growth Of Moulds And Some Bacteria [1]. Propionic Acid (PA) And Its Derivatives Are Largely Used As Feed And Food Derivatives. The Compound Frequently Accompanies Steroid Medications, Including Testosterone. Propionic Acid Is Also Useful As A Chemical Intermediate. It Can Be Used To Modify Synthetic Cellulose Fibres. It Is Also Used To Make Pesticides And Pharmaceuticals. The Esters Of PA Are Sometimes Used As Solvent Or Artificial Flavourings [2]. Physicians Commonly Prescribe The Formulation For Breast Cancer And Hormone Replacement Therapy. It Is Also Used To Make Some Specialized Propionates, Such As Cellulose Acetate Propionate (CAP), Which Is A Useful Thermoplastic [3]. Derivatives Of Propionic Acid Such As Ibuprofen And Fenoprofen Are Widely Used In The Pharmaceutical Industry [4]. Ibuprofen Is A Nonsteroidal Anti-Inflammatory Drug (NSAID) Derivative Of Propionic Acid Used For Relieving Pain And Reducing Inflammation. It Is Also Used For Fever, Mild-To-Moderate Pain, Painful Menstruation, Osteoarthritis, Dental Pain, Headaches And Pain From Kidney Stones. It Is Used For Inflammatory Diseases Such As Juvenile Idiopathic Arthritis And Rheumatoid Arthritis [5].

In The Progressive Studies Of Propionic Acid Herein 3-(4-Methoxybenzoyl) Propionic Acid (MBPA) Has Been Taken As The Object Of Spectral, Structural And Theoretical Investigations Because Of Its Interesting Physicochemical And Biological Properties. Vibrational Spectroscopy Is Used Not Only For The Functional Group Identification Of Organic Compounds, But Also To Investigate The Molecular Confirmation, Reaction Kinetics, Etc. Literature Survey Reveals That The Vibrational Spectra And The Theoretical Calculations Of MBPA Have Not Been Reported Till Date. The Complete Vibrational Analysis Of MBPA Was Performed By Combining The Experimental (FT-IR And Raman) And Theoretical Information Using Pulay's Density Functional Theory (DFT) Based On The Scaled Quantum Mechanical (SQM) Method. The Vibrational Assignments Have Been Performed Based On The Potential Energy Distribution (PED). The Redistribution Of Electron Density (ED) In Various Bonding And Antibonding Orbitals And Delocalization Energies (E²) Has Been Calculated By The Natural Bond Orbital (NBO) Interactions. HOMO-LUMO Analysis Has Been Used To Elucidate Information Regarding Charge Transfer Within The Molecule.

II. Experimental Details

The Compound 3-(4-Methoxybenzoyl) Propionic Acid In The Solid Form Was Purchased From The Sigma Aldrich Chemical Company (USA) With A Stated Purity Of 98% And Used As Such Without Further Purification. FT-Raman Spectra Were Recorded In The Range Of 4000-50cm⁻¹ Using BRUKER, Model RFS 100/S FT-Raman Spectrophotometer. The FT-IR Spectrum Of The Sample Was Recorded Using Perkin Elmer

RXI Spectrometer In The Region 4000-450cm⁻¹ In Evacuation Mode Using Kbr Pellet Technique. The U-V Spectra Were Recorded In The Polar Solvents, Water And Ethanol In The Region 200-400 Nm Using Perkin Elmer LAMDA UV-Vis NIR Spectrometer.

III. Computational Details

The Quantum Chemical Calculations Of MBPA Have Been Performed Using Gaussian 03 Program Package [6] At The Ab Initio HF And Becke 3 – Lee – Yang – Parr (B3LYP) Methods. The Molecular Geometry, Optimized Parameters And Vibrational Frequencies Are Computed By Performing Both Ab Initio (HF) With 6-31G (D,P) And DFT(B3LYP) With 6-31++G(D,P) And 6-311++G(D,P)Basis Sets. The Harmonic Vibrational Frequencies Have Been Analytically Calculated By Taking The Second Order Derivative Of Energy Using The Same Level Of Theory. The Scaling Of The Force Field Was Performed According To The Scaled Quantum Mechanical Procedure (SQM) [7, 8] Using Selective Scaling In The Natural Internal Co-Ordinate Representation [9, 10] To Obtain A Better Agreement Between The Theory And The Experiment. Normal Co-Ordinate Analyses Have Been Performed In Order To Obtain The Detailed Interpretation Of The Fundamental Modes Using The MOLVIB Program Version 7.0 Written By Sundius [11, 12]. The Raman Activities (S_i) Calculated By The Gaussian 03W Program Are Adjusted And Converted Into Relative Raman Intensities (I_i) During The Scaling Program With MOLVIB Using The Following Relationship Derived From The Basic Theory Of Raman Scattering[13,14].

$$I_i = \frac{f(v_o - v_i)^4 S_i}{v_i \left[1 - \exp\left(\frac{-hcv_i}{kT}\right) \right]} \dots \dots (1)$$

Where V₀ Is The Exciting Wavenumber (Cm⁻¹) Of Laser Light Source Used While Recording Raman Spectra, V_iis The Vibrational Wavenumber Of The Ith Normal Mode; H, K, C And T Are Planck And Boltzmann Constants, Speed Of Light And Temperature In Kelvin Respectively. F Is The Suitably Chosen Common Normalization Factor For All The Peak Intensities.

The NBO Calculations [15] Were Performed Using NBO 3.1 Program As Carried Out In The Gaussian 03 W Package At The DFT/B3LYP Level In Order To Understand The Various Second Order Interactions Between The Filled Orbitals Of One Sub System And The Vacant Orbitals Of Another Sub System, Which Is A Measure Of Delocalization Or Hyper Conjugation.

IV. Results And Discussion

4.1. Molecular Geometry

The Optimized Geometry Structure Of The Title Compound Is Shown In Figure. 1. The Optimized Structure Parameters For MBPA Calculated By HF/6-31G (D,P),B3LYP/6-31++G(D,P)Andb3lyp/6-311++G(D,P) Basis Sets Are Listed In Table 1. The Optimized Geometric Parameters Of MBPA Are Compared With The Experimental XRD Data Of The Title Molecule. As Seen From Table 1, Most Of The Optimized Bond Lengths Are Slightly Larger Than The Experimental Values, And The Bond Angles Are Slightly Different From Experimental Values. This Is Due To The Fact That The Experimental Results Belong To Solid Phase And The Theoretical Calculations Belong To Gaseous Phase.

In The Title Molecule, The Introduction Of Two Substituent Groups On The Benzene Ring Causes Some Changes In The C-C Bond Lengths And Also In The Position Of The Substituents In The Benzene Ring. The Values Of C-C Bond Lengths Are In Good Agreement With The Data Obtained For Substituted Benzenes [16]. In The Carboxylic Group, The Calculated Bond Lengths C1-O4 And C1-O5 Of The Title Molecule Are 1.199Å, 1.363Å By B3LYP/6-311++G(D,P) And 1.207Å, 1.364Å By B3LYP/6-31++G(D,P) Method, Which Are In Good Agreement With The Literature Values C=O(1.209 Å) And C-O(1.355 Å)[17]. The Bond Lengths C6=O13(1.221 Å/1.228Å), C7-C6(1.489 Å/1.489Å), C6-C3(1.524Å/1.525Å), C2-C3(1.524 Å/1.525Å) And C2-C1(1.519Å/1.519Å) By B3LYP/6-311++G(D,P)/6-31++G(D,P)Method Are In Good Agreement With The Values Reported For Fenbufen[18].



Fig 1 Molecular Structure With Atom Numbering Of MBPA.

Table 1 Experimental (XRD) And Optimized Geometrical Parameters Of MBPA Computed At HF/6-31G(D,P), B3LYP/6-31++G(D,P) And B3LYP/6-311++G(D,P) Basis Sets.

Bond Length	Experimental Value	Bond Lengths(Å)		
		HF/6-31G(D,P)	B3LYP/6-31++G(D,P)	B3LYP/6-311++G(D,P)
C1-C2	1.491	1.513	1.519	1.519
C1-O4	1.229	1.183	1.207	1.199
C1-O5	1.301	1.334	1.364	1.363
C2-C3	1.511	1.521	1.525	1.524
C3-C6	1.508	1.518	1.525	1.524
O5-H20	0.820	0.944	0.969	0.965
C6-C7	1.478	1.491	1.489	1.489
C6-O13	1.220	1.199	1.228	1.221
C7-C8	1.384	1.388	1.403	1.399
C7-C12	1.397	1.397	1.409	1.406
C8-C9	1.383	1.383	1.392	1.389
C9-C10	1.379	1.390	1.405	1.402
C10-C11	1.395	1.394	1.405	1.402
C10-O14	1.352	1.341	1.359	1.357
C11-C12	1.370	1.375	1.387	1.384
O14-C15	1.426	1.402	1.426	1.425

Bond Angle	Experimental Value	Bond Angles(°)		
		HF/6-31G(D,P)	B3LYP/6-31++G(D,P)	B3LYP/6-311++G(D,P)
C2-C1-O4	122.59	124.618	125.227	125.329
C2-C1-O5	113.76	115.017	115.229	114.976
O4-C1-O5	123.60	120.365	119.544	119.695
C1-C2-C3	113.82	112.386	112.622	112.746
C2-C3-C6	112.19	111.966	112.391	112.423
C1-O5-H20	109.18	112.289	110.931	110.624
C3-C6-C7	118.98	118.689	118.619	118.429
C3-C6-O13	120.04	120.370	120.282	120.409
C7-C6-O13	120.98	120.941	121.099	121.161
C6-C7-C8	121.92	118.434	118.617	118.563
C6-C7-C12	119.76	123.366	123.118	123.204
C8-C7-C12	118.32	118.201	118.265	118.234
C7-C8-C9	121.48	121.585	121.497	121.501
C8-C9-C10	119.26	119.389	119.428	119.479
C9-C10-C11	120.23	119.771	119.823	119.746
C9-C10-O14	124.36	124.466	124.463	124.464

4.2 Potential Energy Scan

The Potential Energy Surface (PES) Scan With The B3LYP/6-311++G(D,P) Level Of The Theoretical Approximations Was Performed For The Title Molecule By Varying The Dihedral Angle (C1-C2-C3-H18) In Steps Of 0°, 10°, 20°, 30°, . . . 360° And The Resultant Minimum Energy Curve As Function Of Dihedral Angle Is Shown In Fig 2. The Dihedral Angle (C1-C2-C3-H18) For MBPA Is Also The Relevant Co-Ordinate For Conformational Flexibility Within The Molecule. All The Geometrical Parameters Were Simultaneously Relaxed During The Calculation. From The Graph, It Is Observed That The Minimum Energies For This Rotation Are Obtained At 0° And 360°, Which Correspond To The Global Minimum Energies – 727.346594 And – 727.346641 Hartrees

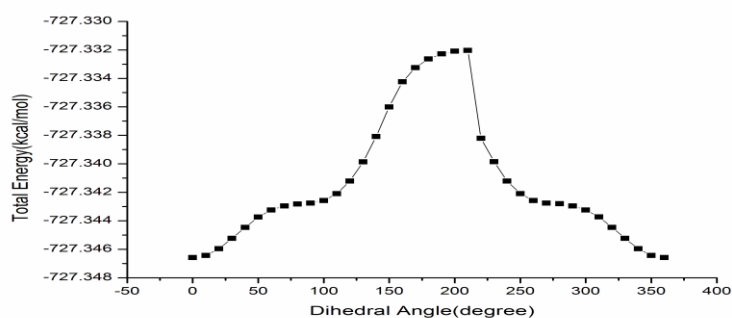


Fig.2 PES Scan For The Selected Torsional Angle T (C1-C2-C3-H18)

4.3. Vibrational Analysis

The Vibrational Spectral Assignments Of MBPA Have Been Carried Out With The Help Of Normal Coordinate Analysis. The Non-Redundant Set Of Local Symmetry Coordinates Are Constructed By Suitable Linear Combinations Of Internal Coordinates Chosen According To The Recommendations Of Pulay Et Al. The Computed Wave Numbers Are Selectively Scaled According To The SQM Procedure Suggested By Rauhut And Pulay [19]. The Detailed Vibrational Spectral Assignments Of The Experimental Wavenumbers Are Based On Normal Mode Analyses And A Comparison With Theoretically Scaled Wavenumbers With PED By HF And B3LYP Methods. The Observed And Scaled Theoretical Frequencies Using HF/6-31G (D,P), B3LYP/6-311++G(D,P) And B3LYP/6-31++G(D,P) Basis Sets With Peds Are Shown In Table 2. The Experimental (FT-IR And FT-Raman) And Simulated Vibrational Spectra Of MBPA Are Displayed In Figures 3.

Table 2. Comparison Of The Experimental (FT-IR And FT-Raman) Wavenumbers (Cm⁻¹) And Theoretical Wavenumbers (Cm⁻¹) Of MBPA Calculated By HF/6-31G (D,P), B3LYP/6-31++G (D,P) And B3LYP/6-311++G (D,P) Basis Sets.

Observed Wavenumbers (Cm ⁻¹)		Calculated By HF/6-31G(D,P)			Calculated By B3LYP/6-31++G(D,P)			Calculated By B3LYP/6-311++G(D,P)			Characterisation Of Normal Modes With PED (%) ^c
		Scale d Wave numbers (Cm ⁻¹)	A _{ir} ^a	I _r ^b	Scale d Wave numbers (Cm ⁻¹)	A _{ir} ^a	I _r ^b	Scaled Wavenumbers (Cm ⁻¹)	A _{ir} ^a	I _r ^b	
IR	Raman										
3318(W)	-	3318	87	41.4	3318	44.3	62.5	3318	50.1	69.8	Yoh(100)
3104(W)	3106(W)	3168	30	118	3207	14.8	118.5	3077	8.3	121.8	Ych(99)
3070(W)	3063(W)	3079	10	109	3077	10.4	125.8	3066	3.6	126.6	Ych(99)
3051(W)	-	3068	7.1	110	3066	4.6	129.8	3059	0.03	41	Ych(98)
-	-	3060	4	43.7	3059	0.3	38.3	3051	3.5	40	Ych(98)
3028(W)	3029(W)	3046	8	44	3050	5.5	43.4	3049	16.3	124	CH3ips(94)
2966(W)	2985(W)	2966	14.4	6.5	2966	9	10.2	2966	6.6	8.6	CH2ASS(87),CH2AS1(12)
-	2954(W)	2951	15.3	46.4	2948	36	63.7	2956	19.1	70.2	CH2SS(98)
2948(W)	-	2948	50	45.2	2936	2.9	71.6	2948	31.5	59.8	CH3ops(100)
2936(W)	-	2936	2.8	76.9	2926	28.8	3.4	2936	2.2	61	CH2AS1(87),CH2ASS(13)
2917(W)	2921(M)	2917	10.6	86.6	2917	0.4	170.2	2917	9.9	121.7	CH2SS1(98)
2841(W)	2841(W)	2841	52.6	128	2841	57.3	176.5	2841	56	192.4	CH3SS(96)
1695(S)	-	1695	239.9	7.6	1695	168.9	17.2	1695	185.4	19.9	Cod2s(79)
1674(W)	1665(S)	1665	148.3	7.1	1674	375.8	274.3	1674	256.9	135.1	Cods(74),Bccc(6)
1599(S)	1605(S)	1630	294.3	183	1599	220.6	123.8	1596	323.7	299.8	Ycc(61), Bch(19)
1574(S)	1576(S)	1606	108.2	52.6	1574	17.6	18.3	1574	20.1	15.3	CH3ipb(94)
1565(S)	-	1572	7.8	25	1551	10.2	11.2	1551	7.6	6	Ycc(67), Bch(11)
1514(S)	1515(W)	1514	135.6	2.2	1514	66.1	19.5	1510	50.1	4.3	Ycc (42), Bch (32), Ycc(9)
1464(M)	1463(W)	1465	16.5	13.8	1464	35.5	13.8	1464	31.4	10	CH3opb(89), CH3ipr(8)
1425(S)	1439(W)	1435	2.4	10.1	1435	32.1	6.5	1435	1.9	5.1	CH3sb(87), Bch(5)
1406(S)	1406(W)	1411	12.9	1.2	1406	11.6	4.7	1406	12.8	3.2	CH2SC(83)
1396(S)	1396(W)	1405	1	3.1	1397	58.3	3.2	1402	10.6	1.8	Ycc(49), Bch(34)
1361(S)	-	1398	0.8	5	1389	14.3	5	1361	15.6	3.7	CH2wag1(66), Ycc1(17)
1317(M)	1320(W)	1379	15.4	1.7	1360	304.2	6.3	1323	347.1	48.3	Ycc(25), Ccar(22)
1302(M)	-	1361	3.9	11.4	1320	137.8	15	1302	0.3	6.9	CH2tw1(84), CH2tw(7)
1298(M)	-	1313	467.	39.8	1302	0.2	8.5	1296	16.9	1.1	Bch(36), Ycc(31)

			7								
1266(M)	1269(W)	1302	6.8	15.3	1288	19	11.5	1272	87.7	18.2	Bch(44), Ycc(28)
1246(S)	1245(S)	1285	172.7	38	1246	121.5	13.5	1247	149.9	10.7	Yco(41), Ycc(28)
1240(W)	-	1247	428.4	3.4	1220	396	6.2	1242	190.6	2.7	CH2sc1(73), Bhoc(10)
1220(S)	1220(M)	1214	35.2	22.6	1217	45.5	0.1	1220	317.1	8.8	Bhoc(58), CH2sc1(15)
1189(S)	1190(M)	1197	24.4	7.7	1211	1.3	2.7	1181	11.5	13.4	CH2wag(53), Ycc1(8)
1173(S)	1181(M)	1189	2.7	8.3	1181	10.8	6.1	1173	0.4	2.9	CH3ipr(72), Ycc(8)
1161(M)	-	1150	0.5	6.6	1173	5.9	4.7	1159	189.2	39.3	Bch(59), Ycc(15)
1112(M)	1115(W)	1115	3	2.5	1115	0	0.7	1115	0.9	3.2	CH3opr(96)
1109(M)	-	1098	90.5	12	1100	81.3	8.8	1109	6.6	0.7	Bch(63), Ycc(26)
1064(M)	1065(W)	1051	21.2	1.8	1064	3.8	4.1	1065	79.5	18.7	Ycc(32), Yco2(28)
1058(W)	-	1026	113.3	1.3	1052	18.3	1.1	1057	0.2	0.8	CH2tw(53), CH2tw1(18)
1027(S)	1025(W)	1020	4.6	10	1027	144.5	3.6	1025	98.9	1.1	Ycc1(38), Yco2(28)
1007(W)	1007(W)	992	2	2.8	1007	76.5	1	1007	86.8	1.5	Yco1(73), Ycc(11)
999(M)	-	980	145.7	14.9	992	0	1.2	1004	0.4	1.6	Bring1(46), Ycc(34)
992(M)	994(W)	963	198.5	1.5	983	0.1	0.8	992	0.7	2	CH2ro1(35), CH2ro(21)
968(M)	-	959	0.5	0.1	966	15.7	3.8	958	0.8	0.04	Γch(91), Γring1(13)
-	955(W)	940	0	0.6	960	0.4	0.2	953	39.7	3.7	Ycc1(38), Bccc(20)
937(S)	942(W)	925	10.1	1.5	933	0	0.1	937	0	0	Γch(84), Γring1(13)
854(W)	855(W)	849	28.9	19.7	854	37.5	26.5	855	21.2	28.7	Ycc1(50), CCSC1(13)
833(S)	831(W)	833	18.6	0.5	832	50.5	0.4	833	44.3	0.1	Γ CH(60), Γco(18),
-	808(M)	804	10	2.7	809	9.8	36.5	805	10.1	31.3	Ycc(30), Bring1(22)
804(M)	-	803	62.1	2.5	804	0.2	0.8	804	0.2	0.1	Γ CH(99)
-	-	794	30.4	10.4	765	16	0.1	772	19.9	0.3	CH2ro(24), CH2ro(24)
735(W)	735(W)	725	49.5	2.6	738	3.9	0.1	737	5	0.5	Ycc1(27)
721(W)	722(W)	722	5.4	0.6	722	1.4	0.5	721	3.4	0.4	Γ Ring1(60)
634(W)	635(S)	627	17	1.1	633	4	8.1	635	2.6	7.1	Bring1(82)
613(M)	614(W)	601	1	7.6	614	25.9	3	612	21.8	2.5	Bcoo(39)
577(M)	-	574	57.7	1.3	576	52.7	1.3	578	39.2	0.4	Boc(26)
553(S)	-	553	24.6	0.1	554	22.7	0.1	553	19.6	0.1	Γccar(23)
521(S)	-	521	3.4	0.6	521	29.2	0.9	521	34.3	0.7	Γcc(40), Toh(30)
503(W)	515(W)	516	7	2	515	0.1	0.4	515	6.4	2.2	Bccc(29)
484(W)	-	483	0.8	0.7	484	1.5	0.8	484	1.41	0.5	Γring1(30)
464(W)	-	460	3.4	1.2	455	3.5	4.4	458	5.6	3.7	Bcoc(33)
-	417(W)	419	1.9	0.1	417	66.4	1.7	417	72.2	0.7	Toh(46)
-	-	417	121.4	1.7	411	0	0	409	0.4	0.02	Γring1(78)
-	-	377	3.6	0.3	379	3	1.5	377	3.6	2.2	Bcoc(32)
-	332(W)	321	2.2	2	331	2.2	1.8	325	1.7	1.8	Bccar(23)
-	295(S)	294	1.1	2.2	291	1.4	1.3	295	1.4	0.8	Bring1(34), Tch3(22)
-	239(W)	241	0.5	0.4	238	0.1	1.5	238	0.5	0.4	CCSC2(21), Bco(20)
-	-	226	0	0.5	226	0	1.3	229	0	1.7	Tch3(65)
-	-	210	7.7	3.1	201	2.3	4	207	7.1	4	CCSC1(21), Ycc1(19)
-	165(W)	161	22.6	0.4	167	24.8	0.3	162	18.4	1	Bco(26), CCSC2(24)
-	129(W)	129	1.7	1	129	2.8	0.4	129	3.9	0.4	Tco(53)
-	84(Vs)	86	0.2	0	87	0.6	0.5	84	0.2	0.7	Γring1(24), Tcc(24)
-	-	84	16.5	0.1	77	0	0.6	65	7.3	0.2	Tcc(34)
-	-	71	0	0.9	64	5.4	0.4	61	3.5	0.7	CCSC1(30)
-	-	66	4.1	0.5	55	3.8	0.7	42	1.8	0.5	Tch21(33)
-	-	31	6.4	1.1	28	1.3	2.7	26	0	1.6	Tch23(23)
-	-	24	4.9	2	1	0	0.4	8	11.8	0.5	Tch22(45)

Vs – Very Strong ; S – Strong; M- Medium; W – Weak; AS- Asymmetric; SS – Symmetric; Y – Stretching; B – In-Plane Bending; Γ – Out-Of- Plane Bending; T – Torsion; Sc – Scissoring; Ro – Rocking; Wag – Wagging; Tw – Twisting; Sb – Symmetric Bending; Ips – In-Plane Stretching; Ops – Out-Of-Plane Stretching; Ipb – In-Plane Bending; Opb – Out-Of-Plane Bending; Ipr – In-Plane Rocking; Opr – Out-Of-Plane Rocking;

^Acalculated IR Intensities.

^BRaman Activity.

^Conly PED Values Greater Than 10% Are Given.

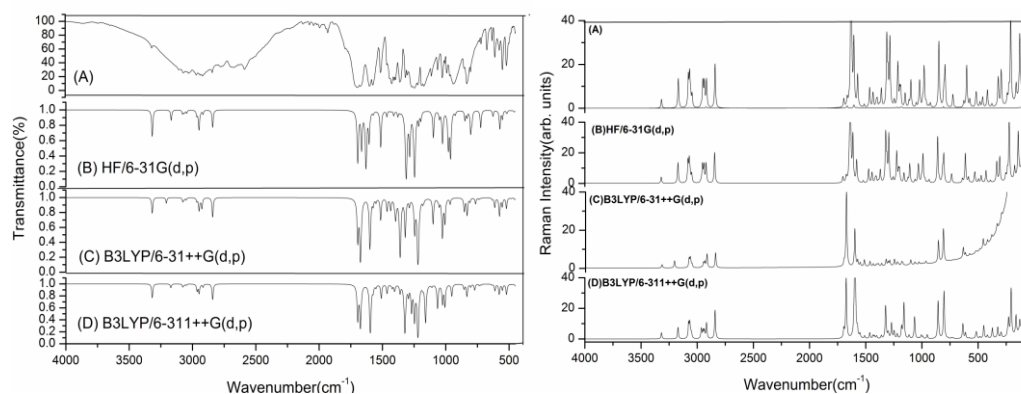


Fig.3 Experimental (A), Simulated (B), (C) And (D) Infrared Spectra Raman Spectra Of MBPA At HF/6-31G(D,P), B3LYP/6-31++G(D,P) And B3LYP/6-311++G(D,P) Levels.

4.3.1. C-H Vibrations

In The Hetero Aromatic Compounds, The C-H Stretching Vibrations Normally Occur At 3100-3000 cm^{-1} [20]. In This Region, These Vibrations Are Not Found To Be Affected By The Nature And Position Of The Substituent [21]. In MBPA, The FT-IR Bands At 3104, 3070 And 3051 cm^{-1} And The FT-Raman Bands At 3106 And 3063 cm^{-1} Have Been Assigned To C-H Stretching Vibrations. Most Of The C-H Stretching Modes Are Found To Be Weak Which Is Due To The Charge Transfer From The Hydrogen Atoms To The Carbon Atoms. The C-H Stretching Vibrations Are Calculated At 3168, 3079, 3068 And 3060 cm^{-1} by HF/6-31 G(D,P) Method And At 3207, 3077, 3066 And 3059 cm^{-1} By B3LYP/6-31++G (D,P) Method And At 3077, 3066, 3059 And 3051 cm^{-1} by B3LYP/6-311++G (D,P) Method. The C-H In-Plane Bending Vibrations Usually Occur In The Region 1300-1000 cm^{-1} And These Vibrations Are Very Useful For Characterization Purposes [22]. The C-H Out-Of-Plane Bending Frequencies Appear In The Range Of 750-1000 cm^{-1} [23]. The C-H In-Plane Bending Vibrations Are Computed Theoretically At 1313, 1302, 1150, 1098 And 1302, 1288, 1173, 1100 cm^{-1} and 1296, 1272, 1159, 1109 cm^{-1} by HF/6-31G(D,P), B3LYP/6-31++G(D,P) And B3LYP/6-311++G (D,P) Methods Respectively. Medium Peaks At 1298, 1266, 1161 And 1109 cm^{-1} In The FT-IR And At 1269 cm^{-1} In The FT-Raman Spectrum Of MBPA Occur Due To C-H In-Plane Bending Vibrations. The Calculated Values For C-H Out-Of-Plane Bending Vibrations Are At 959, 925, 833, 803 cm^{-1} By HF/6-31G (D,P) And At 966, 933, 832, 804 cm^{-1} By B3LYP/6-31++G(D,P) And At 958, 937, 833, 804 cm^{-1} By B3LYP/6-311++G(D,P) Method. The C-H Out-Of Plane Bending Vibrations Observed In FT-IR At 968, 937, 833 And 804 cm^{-1} and In FT-Raman At 942 And 831 cm^{-1} are In Agreement With The Theoretical Values.

4.3.2. C-C Vibrations

The Ring Carbon-Carbon Stretching Vibrations Occur In The Region 1305 \pm 25 – 1590 \pm 40 cm^{-1} [24, 21]. The C-C Stretching Vibrations Of MBPA Are Observed At 1599, 1565, 1514, 1396, 1317 And 1064 cm^{-1} In The FT-IR Spectrum And At 1605, 1515, 1396, 1320 And 1065 cm^{-1} In The FT Raman Spectrum. The Computed Wavenumber For C-C Vibrations Are Found At 1630, 1572, 1514, 1405, 1379, 1051 cm^{-1} By HF/6-31G(D,P) Method, 1599, 1551, 1514, 1397, 1360, 1064 cm^{-1} By B3LYP/6-31++G(D, P) Method And At 1596, 1551, 1510, 1402, 1323, 1065 cm^{-1} By b3lyp/6-311++G(D, P) Method. The Observed Values Are In Good Correlation With The Calculated Values. For Di-Substituted Benzenes, The Bands Due To The In-Plane Ring Deformation Vibration And Out-Of-Plane Ring Deformation Vibration Occur In The Region 620 \pm 15– 270 \pm 115 cm^{-1} And 700 \pm 25 – 395 \pm 15 cm^{-1} Respectively [24, 25]. The In-Plane Ring Deformation Vibrations Of MBPA Are Observed At 999 And 634 cm^{-1} In The FTIR And At 635 And 295 cm^{-1} In The FT-Raman Spectrum. The Out-Of-Plane Ring Deformation Vibrations Appear At 721 And 484 cm^{-1} As Strong To Medium Band In The FT-IR Spectrum And At 722 cm^{-1} In The Raman Spectrum. The Calculated C-C-C In-Plane Bending Vibrations Are Found At 980, 627, 294 cm^{-1} By HF/6-31G(D,P) And At 992, 633, 291 cm^{-1} by B3LYP/6-31++G(D,P) And At 1004, 635, 295 cm^{-1} B3LYP/6-311++G(D, P) Method. The C-C-C Out-Of-Plane Bending Vibrations Are Theoretically Computed At 722, 483, 417 cm^{-1} By HF/6-31G(D,P) And At 722, 484, 411 cm^{-1} by b3lyp/6-31++G(D, P) And At 721, 484, 409 cm^{-1} By B3LYP/6-311++G(D, P) Method.

4.3.3. Methoxy Group Vibrations

For O-CH₃ Compound, The C-H Asymmetric And Symmetric Stretching Vibrations Appear In The Range 3100 – 2900 cm^{-1} And 2900 – 2800 cm^{-1} Respectively [26, 27]. The CH₃ Asymmetric Stretching Vibrations Appear As Weak Bands In The FT IR Spectrum At 3028 And 2948 cm^{-1} And In The Raman Spectrum At 3029 cm^{-1} . The Symmetric CH₃ stretching Vibration Is Observed As A Weak Band In The IR Spectrum At 2841 cm^{-1} and The Raman Band At 2841 cm^{-1} For The Title Molecule. The Theoretically Computed

CH₃ Asymmetric And Symmetric Stretching Vibrations Assigned At 3046, 2948 And 2841cm⁻¹ By HF/6-31G(D,P) And At 3050,2936 And 2841cm⁻¹ by B3LYP/6-31++G(D,P) And The Bands At 3049, 2948 And 2841cm⁻¹ By B3LYP/6-311++G(D,P) Method Show Excellent Agreement With The Experimental Values. The Asymmetric And Symmetric Bending Vibrations Of CH₃ Group Usually Appear In The Range Of 1550-1410 Cm⁻¹ For Methyl Substituted Benzenes [28]. In The Title Compound, Strong And Medium Intensity Bands Appeared At 1574 Cm⁻¹ And 1464 Cm⁻¹ In The FT-IR Are Assigned To CH₃ Asymmetric Deformation Vibration. In The Raman Spectrum, The Bands Are Observed At 1576 Cm⁻¹ And 1463 Cm⁻¹. The Theoretically Calculated Values Are At 1606, 1465cm⁻¹ By HF/6-31G(D,P) And At 1574, 1464cm⁻¹ By Both B3LYP/6-311++G(D,P) And The B3LYP/6-31++G(D,P) Methods Coincide Very Well With The Experimental Values. The CH₃ Symmetric Deformations Are Observed At 1425 Cm⁻¹ In FT-IR And At 1439 Cm⁻¹ In The Raman Spectrum. The HF/6-31G(D,P), B3LYP/6-31++G(D,P) And B3LYP/6-311++G(D,P) Calculations Give Symmetric CH₃ Deformations At 1435cm⁻¹ for The Title Compound. The Rocking Vibrations Of The CH₃ Group Have Been Calculated At 1189, 1115 Cm⁻¹ By HF/6-31G(D,P) And At 1181, 1115cm⁻¹ B3LYP/6-31++G(D,P) And At 1173,1115cm⁻¹ By B3LYP/6-311++G(D,P) Method, Which Also Show Good Agreement With The FT-IR And Raman Recorded Values At 1173 Cm⁻¹, 1112cm⁻¹ And 1181 Cm⁻¹, 1115 Cm⁻¹ for MBPA Respectively. The O-CH₃ Stretching Mode Is Normally Assigned In The Region 1000-1100 Cm⁻¹ [29-31] For Anisole And Its Derivatives. In MBPA, A Weak Band Is Found At 1007 Cm⁻¹ For O-CH₃ Stretching Vibration In The FT-IR And Raman Spectra. The Theoretically Computed Value At 992cm⁻¹ by HF/6-31G(D,P) And At 1007cm⁻¹ By Both B3LYP/6-31++G(D,P), B3LYP/6-311++G(D,P) Methods For O-CH₃ Stretching Coincides With The Experimental Values. Raman Rao Et Al. [32] Have Proposed Assignment For C-O-CH₃ Mode In The Region 300-670 Cm⁻¹. In Accordance With The Above A Band Is Assigned To The Theoretically Calculated Value By HF/6-31G(D,P) At 460cm⁻¹ And By B3LYP/6-31++G(D,P) At 455cm⁻¹ And By B3LYP/6-311++G(D,P) At 458cm⁻¹ As C-O-CH₃ Bending Mode, Which Exactly Coincides With The 464 Cm⁻¹ Band Observed In The FT-IR Spectrum. A Strong Band Is Observed In The Region 1300-1200 Cm⁻¹ Due To C-O Stretching Vibrations [33]. In The Title Compound, A Strong Band Assigned At 1246 Cm⁻¹ And 1245 Cm⁻¹ In The FT-IR And Raman Spectra For C-O Stretching Vibrations. The Theoretical Value Of C-O Stretching Vibration Is Calculated At 1285cm⁻¹ By HF/6-31G(D,P) And At 1246cm⁻¹ By B3LYP/6-31++G(D,P) And At 1247cm⁻¹ By B3LYP/6-311++G(D,P) Method. The C-O In Plane Bending Vibration Is Found At 165 Cm⁻¹ In The Raman Spectrum And These Assignments Are Also Supported By The Literature [34]. The Torsion Mode Of The O-CH₃ Group Was Observed For Anisole At 100 Cm⁻¹. The Computed Value Predicted By The HF/6-31G (D,P), B3LYP/6-31++G(D,P) And B3LYP/6-311++G(D,P) Methods Is 129 Cm⁻¹ And It Correlates With The Experimental Observation For The O-CH₃ Torsion Mode For MBPA.

4.3.4. Methylene Group Vibrations

The CH₂ Group Frequencies, Basically Six Fundamentals Can Be Associated, Namely With Symmetric, Asymmetric, Scissoring, Rocking, Wagging And Twisting Vibrations. The Methylene Asymmetric Stretching Is Found At 2980±45 Cm⁻¹ And The Symmetric Stretching At 2920±45 Cm⁻¹. In The MBPA Molecule, The Computed Wavenumbers At 2966, 2951cm⁻¹ By HF/6-31G(D,P) Method And At 2966, 2948 Cm⁻¹ By B3LYP/6-31++G(D, P) Method And At 2966, 2956cm⁻¹ By B3LYP/6-311++G(D,P) Method Are Assigned To CH₂(1) Asymmetric And Symmetric Stretching Vibrations. In The Present Work, The Strong Band Observed At 2966 Cm⁻¹ In The FT-IR And A Medium Band Observed At 2985 Cm⁻¹ In The FT-Raman Of MBPA Are Assigned To The CH₂ Asymmetric Modes Of Vibrations. Similarly, The Band At 2954cm⁻¹ in The FT-Raman Of MBPA Is Assigned To The Symmetric Stretching Modes Of Vibrations. The Methylene(COOH) Asymmetric Stretching Is Found At 2950±30 Cm⁻¹ And The Symmetric Stretching At 2885±45 Cm⁻¹ [24, 35]. The Bands At 2936cm⁻¹ and 2917cm⁻¹ are Assigned To CH₂(2) Asymmetric And Symmetric Vibrations In The FT-IR Spectrum And The Band At 2921cm⁻¹ is Assigned To Symmetric Vibration In Raman, Which Are In Good Agreement With The Calculated Values At 2936cm⁻¹ and 2917cm⁻¹ By HF/6-31G(D,P) And B3LYP/6-311++G(D,P) Methods And At 2926 And 2917cm⁻¹ By B3LYP/6-31++G(D,P) Method. The Methylene Deformation Of -CH₂CH₂OH Compounds Absorbs In The Region 1435±25cm⁻¹ With Moderate Intensity [36]. In The MBPA Molecule, The Δch₂ Vibration Is Observed At 1406 Cm⁻¹ As Strong Band In The FT-IR And At 1406cm⁻¹ As Weak Band In The FT-Raman Spectrum, Which Agrees Well With The Computed Wavenumbers At 1411cm⁻¹ By HF/6-31G(D,P) And At 1406 Cm⁻¹ By The B3LYP/6-31++G(D, P) And B3LYP/6-311++G(D,P) Methods. The Methylene And Methylene (COOH) Wags Absorb With A Weak To Moderate Intensity In The Region 1260±90 Cm⁻¹ And 1360±30cm⁻¹ [37,38]. For The MBPA Molecule, The Wagging Vibrational Band Of CH₂ Mode Is Observed At 1189cm⁻¹ As Strong Band In The FT-IR And At 1190 Cm⁻¹ As Medium Band In The FT-Raman. The Theoretically Computed CH₂ Wagging Vibration At 1197cm⁻¹ By HF/6-31G(D,P) And At 1211cm⁻¹ By B3LYP/6-31++G(D,P) Method And At 1181 Cm⁻¹ By B3LYP/6-311++G (D,P) Level Which Shows Good Agreement With The Experimental Observation. Similarly, CH₂ (COOH) Wagging Vibration Is Observed At 1361cm⁻¹ as Strong Band In FT-IR, Which Shows Good Agreement With The

Computed Value At 1398cm^{-1} By HF/6-31G(D,P) And At 1389cm^{-1} By B3LYP/6-31++G(D,P) And At 1361cm^{-1} By B3LYP/6-311++G(D,P) Method. The Weak To Moderate Bands At $1210\pm 80\text{cm}^{-1}$ and $1240\pm 60\text{cm}^{-1}$ are assigned To The Methylene And Methylene (COOH) Twist Modes. The Twisting Vibrations Of MBPA Are Observed At 1302cm^{-1} and 1058cm^{-1} as Medium Bands In The FT-IR Spectrum. The Computed Wavenumbers For The Twisting Modes Are Assigned At $1361, 1026\text{cm}^{-1}$ By HF/6-31G (D,P) And At $1320, 1052\text{cm}^{-1}$ By B3LYP/6-31++G (D, P) And At $1302, 1057\text{cm}^{-1}$ By B3LYP/6-311++G(D,P) Method. The Methylene Rocking Vibrations Absorb In The Region $820\pm 70\text{cm}^{-1}$ and $900\pm 60\text{cm}^{-1}$ With Band Intensities Varying From Weak To Moderate [24, 39, 40]. The CH_2 (COOH) Rocking Vibration Of MBPA Is Observed At 992cm^{-1} In The FT-IR Spectrum And At 994cm^{-1} In The Raman Spectrum. The Corresponding Calculated Wavenumber Is At 963cm^{-1} by HF/6-31G (D,P) And At 983cm^{-1} By B3LYP/6-31++G(D,P) And At 992cm^{-1} By B3lyp/6-311++G (D, P) Basis Set.

4.3.5. COOH Vibrations

The Carboxylic Acid O-H Stretching Is Characterized By A Very Broad Band Appearing Near About $3400\text{-}3600\text{cm}^{-1}$ [41]. The O-H Stretching Band Is Observed At 3318cm^{-1} In The FT-IR Spectrum For The Title Compound. The Band Is Calculated At 3318cm^{-1} By HF/6-31G(D,P), B3LYP/6-31++G(D,P) And B3lyp/6-311++G(D,P) Methods. The In Plane O-H Deformation Vibration Usually Appears As Strong Band In The Region $1445\text{-}1260\text{cm}^{-1}$ [42]. The Theoretically Predicted Band At 1214cm^{-1} in HF/6-31G(D,P) And At 1220cm^{-1} In B3LYP/6-31++G(D,P) And At 1217cm^{-1} In B3LYP/6-311++G(D,P) Method Is Assigned To O-H In Plane Bending Vibration For The Title Molecule And It Is In Good Agreement With The Recorded FT-IR And Raman Spectra At 1220cm^{-1} . The Out-Of-Plane Vibration Lies In The Range $600\text{-}720\text{cm}^{-1}$. The Observed Band Is Assigned At 417cm^{-1} In The Raman Spectrum To O-H Out-Of-Plane Bending. The Theoretically Calculated Values Are At 419cm^{-1} By HF/6-31G(D,P) And At 417cm^{-1} By Both Methods B3LYP/6-31++G(D,P), B3LYP/6-311++G(D,P) For O-H Out-Of-Plane Bending.

The Vibrational Analysis Of The Carboxylic Acid Group Is Made On The Basis Of Carbonyl Group And Hydroxyl Group. The C=O Stretch Of Carboxylic Acid Is Identical To The C=O Stretch In Ketones, Which Is Expected In The Region $1740\text{-}1660\text{cm}^{-1}$ [43]. In The Title Molecule, The $\text{N}_{\text{C=O(Carbonyl)}}$ Frequency Is Observed At 1674cm^{-1} in FT-IR Spectrum And At 1665cm^{-1} As Strong Band In FT-Raman Spectrum. The Calculated Stretching Vibration Mode Of The C=O(Carbonyl) Band For MBPA Is At 1665cm^{-1} By HF/6-31G (D,P) And At 1674cm^{-1} By B3LYP/6-31++G(D,P), B3LYP/6-311++G(D,P) Methods. It Can Also Be Seen From The Observed FT-IR Spectrum That The Stretching Vibration Mode Of The Strongest Band Which Is Assigned To The $\text{N}_{\text{C=O(COOH)}}$ Is 1695cm^{-1} , The Calculated Value Is 1695cm^{-1} By HF/6-31G(D,P), B3LYP/6-31++G(D,P) And B3LYP/6-311++G(D,P) Methods. The C=O(Carbonyl) In-Plane-Deformation Can Be Found In The Extensive Region $550\pm 220\text{cm}^{-1}$ As A Weak To Moderate Absorption [22]. The Band Occurring At 577cm^{-1} In The IR Spectrum Is Assigned To The C=O In-Plane Deformation Mode Of MBPA. The Computed Wavenumber For C=O In-Plane Deformation Mode Is At 574cm^{-1} By HF/6-31G (D,P) And At 576cm^{-1} By B3LYP/6-31++G(D,P) And At 578cm^{-1} By B3LYP/6-311++G(D,P) Method.

4.4. Natural Bond Orbital (NBO) Analysis

The Natural Bond Orbital (NBO) Calculation Was Performed Using The NBO 3.1 Program Implemented In The Gaussian 03 Package At The DFT/B3LYP/6-311++G(D,P) Level In Order To Understand The Various Second-Order Interactions Between The Filled Orbitals And The Vacant Orbitals, Which Is A Measure Of The Delocalization Or Hyper Conjugation. The Hyperconjugative Interaction Energy Was Deduced From The Second-Order Perturbation Approach [44]. The Individual Orbital Energy, The Energy Gap And The Energetic Stabilization Due To Hyperconjugation Interaction Have Been Computed Using The Second-Order Perturbation Approach Which Can Be Given As,

$$E^{(2)} = \Delta e_{ij} = Q_i F(I,J)^2 / (E_j - E_i)$$

Where Q_i Is The Donor Orbital Occupancy, E_j And E_i Are Diagonal Elements (Orbital Energies) And $F(I,J)$ Is The Off Diagonal NBO Fock Matrix Elements.

The Larger The Stabilization Energy Value, The More Intensive Is The Interaction Between The Electron Donors And The Electron Acceptors And The Greater Is The Extent Of Conjugation Of The Whole System. The Possible Intensive Interactions Are Given In Table 3. There Occurs A Strong Intermolecular Hyper-Conjugative Interaction Of C9 - C10 From O14 Of N2 (O14) \rightarrow Π^* (C9- C10) Which Increases ED(0.39703e) That Weakens The Respective Bonds C9- C10 Leading To Stabilization Of 31.92kcal/Mol And Also The Hyper-Conjugative Interaction Of C1 - O4 From O5 Of N2(O5) \rightarrow Π^* (C1- O4) Which Increases ED(0.19669e) That Weakens The Respective Bonds C1- O4 Leading To The Stabilization Of 41.52kcal/Mol. Then The Hyper-Conjugative Interaction Of C1 - O5 From O4 Of N2 (O4) \rightarrow Σ^* (C1-O5) Which Increases ED (0.10089e) That Weakens The Respective Bonds C1 - O5 Leading To The Stabilization Of 33.88kcal/Mol And Also Hyper-Conjugative Interaction Of C2 - C3 From O13 Of N2 (O13) \rightarrow Σ^* (C2-C3) Which Increases ED

(0.05926e) That Weakens The Respective Bonds C2 – C3 Leading To The Stabilization Of 20.85kcal/Mol. The Other Significant Interactions Giving Stronger Stabilization To The Structure Are $\Pi(C7-C8) \rightarrow \Pi^*(C11-C12)$, $\Pi(C11-C12) \rightarrow \Pi^*(C9-C10)$, $\Pi(C9-C10) \rightarrow \Pi^*(C7-C8)$ And $\Pi(C7-C8) \rightarrow \Pi^*(C6-O13)$ With Energies 22.85, 22.63, 25.49 And 20.70kcal/Mol Respectively. These Interactions Are Observed As An Increase In Electron Density (ED) In C – C And C – O Antibonding Orbitals That Weaken The Respective Bonds.

Table 3. Second Order Perturbation Theory Analysis Of Fock Matrix In NBO Basis For MBPA

Donor(I)	ED(I)(E)	Acceptor (J)	ED (J) (E)	E(2)(Kj Mol ⁻¹)	E(J)-E(I) (A.U)	F(I,J) (A.U)
$\Sigma(C3-C6)$	1.98072	$\Sigma^*(C7-C8)$	0.02250	2.32	1.20	0.047
		$\Pi^*(C6-O13)$	0.15783	4.73	0.52	0.046
$\Sigma(O5-H20)$	1.98536	$\Sigma^*(C1-O4)$	0.01856	4.82	1.40	0.073
$\Sigma(C6-C7)$	1.97691	$\Sigma^*(C7-C8)$	0.02250	2.08	1.23	0.045
		$\Sigma^*(C8-C9)$	0.01321	2.31	1.24	0.048
$\Pi(C6-O13)$	1.97506	$\Pi^*(C7-C8)$	0.37683	3.47	0.40	0.037
$\Sigma(C7-C8)$	1.97305	$\Sigma^*(C3-C6)$	0.05926	2.04	1.07	0.042
		$\Sigma^*(C6-C7)$	0.06310	2.31	1.12	0.046
		$\Sigma^*(C7-C12)$	0.02335	3.84	1.26	0.062
		$\Sigma^*(C8-C9)$	0.01321	2.76	1.28	0.053
$\Pi(C7-C8)$	1.62941	$\Pi^*(C6-O13)$	0.15783	20.70	0.27	0.071
		$\Pi^*(C9-C10)$	0.39203	16.88	0.27	0.060
		$\Pi^*(C11-C12)$	0.29522	22.85	0.28	0.072
$\Sigma(C7-C12)$	1.97449	$\Sigma^*(C7-C8)$	0.02250	3.92	1.27	0.063
$\Sigma(C8-C9)$	1.97551	$\Sigma^*(C6-C7)$	0.06310	2.71	1.13	0.050
		$\Sigma^*(C10-O14)$	0.02987	4.47	1.07	0.062
$\Sigma(C8-H21)$	1.97770	$\Sigma^*(C7-C12)$	0.02335	4.64	1.08	0.063
		$\Sigma^*(C9-C10)$	0.02998	3.91	1.06	0.058
$\Sigma(C9-C10)$	1.97845	$\Sigma^*(C8-C9)$	0.01321	3.03	1.30	0.056
		$\Sigma^*(C10-C11)$	0.02314	3.85	1.27	0.062
$\Pi(C9-C10)$	1.62891	$\Pi^*(C7-C8)$	0.37683	25.49	0.30	0.078
		$\Pi^*(C11-C12)$	0.29522	14.95	0.29	0.060
$\Sigma(C9-H22)$	1.97685	$\Sigma^*(C7-C8)$	0.02250	3.70	1.10	0.057
		$\Sigma^*(C10-C11)$	0.02314	3.86	1.08	0.058
$\Sigma(C11-C12)$	1.97661	$\Sigma^*(C6-C7)$	0.06310	3.14	1.14	0.054
		$\Sigma^*(C7-C12)$	0.02335	3.25	1.27	0.057
		$\Sigma^*(C10-C11)$	0.02314	2.65	1.26	0.052
		$\Sigma^*(C10-O14)$	0.02987	3.26	1.07	0.053
$\Pi(C11-C12)$	1.70568	$\Pi^*(C7-C8)$	0.37683	15.76	0.29	0.062
		$\Pi^*(C9-C10)$	0.39203	22.63	0.28	0.072
$\Sigma(O14-C15)$	1.99301	$\Sigma^*(C10-C11)$	0.02314	2.69	1.38	0.055
LP(1)O4	1.97950	$\Sigma^*(C1-C2)$	0.06554	2.44	1.06	0.046
LP(2)O4	1.84483	$\Sigma^*(C1-C2)$	0.06554	18.68	0.63	0.099
		$\Sigma^*(C1-O5)$	0.10089	33.88	0.60	0.129
LP(1)O5	1.97726	$\Sigma^*(C1-C2)$	0.06554	4.48	0.99	0.060
LP(2)O5	1.83402	$\Pi^*(C1-O4)$	0.19669	41.52	0.35	0.109
LP(1)O13	1.97909	$\Sigma^*(C6-C7)$	0.06310	1.40	1.11	0.036
LP(2)O13	1.89285	$\Sigma^*(C3-C6)$	0.05926	20.85	0.64	0.105
		$\Sigma^*(C6-C7)$	0.06310	19.07	0.69	0.104
LP(1)O14	1.96347	$\Sigma^*(C9-C10)$	0.02998	6.95	1.10	0.078
LP(2)O14	1.82772	$\Pi^*(C9-C10)$	0.39203	31.92	0.34	0.098
		$\Sigma^*(C15-H26)$	0.01766	5.38	0.69	0.057
		$\Sigma^*(C15-H27)$	0.01766	5.38	0.69	0.057

^e(2) Means Energy Of Hyper Conjugative Interactions

^A Energy Difference Between Donor And Acceptor I And J NBO Orbitals

^C_f(I,J) Is The Fock Matrix Element Between I And J NBO Orbitals

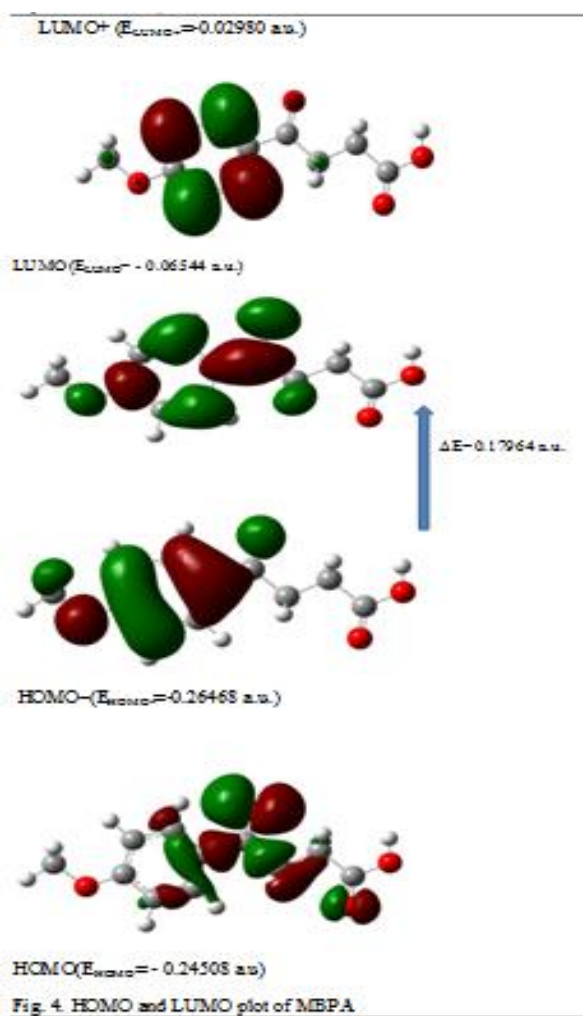
4.5. HOMO-LUMO Analysis

The HOMO And The LUMO Are Very Important Parameters For Chemical Reaction Which Examine The Molecular Orbital For The Title Molecule. The HOMO Is The Orbital That Primarily Acts As An Electron Donor (Highest Occupied MO) And The LUMO Is The Orbital That Acts As The Electron Acceptor (Lowest Unoccupied MO) And The Gap Between HOMO And LUMO Characterizes The Molecular Chemical Stability. The Energy Gap Between The Highest Occupied And The Lowest Unoccupied Molecular Orbital Is A Critical Parameter In Determining The Molecular Electrical Transport Properties Because It Is A Measure Of Electron Conductivity. The HOMO-LUMO Energy Gap Of MBPA Has Been Calculated At The B3LYP/6-311++G (D,P) Level, And It Is 0.17964 A.U. That Reflects The Chemical Activity Of The Molecules. In The Title Molecule, As Shown In Figure 4, The HOMO \rightarrow LUMO Transition Implies That The HOMO Electrons

Located Over The Benzene Ring Extended With The Methoxy Group To The LUMO Electrons Resides Over The Benzene Ring Extended With The Carbonyl Group.

4.6. Molecular Electrostatic Potential

The Molecular Electrostatic Potential (MESP) is widely used as a reactivity map displaying the most probable regions for the electrophilic attack of charged point-like reagents on organic molecules [45]. The MEP is a plot of electrostatic potential onto the constant electron density surface. The different values of the electrostatic potential at the surface are represented by different colours; red represents the regions of the most negative electrostatic potential, blue represents the regions of the most positive electrostatic potential, and green represents the regions of zero potential. The regions of negative potential are usually with the lone pair of electronegative atoms. The MESP of the title compound is obtained based on the B3LYP/6-311++G(D,P) optimized result and shown in Figure 5. As can be seen from the MESP map of the title compound, while regions having the negative potential are over the electronegative atom (oxygen atoms), the regions having the positive potential are over the hydrogen atoms. The red colour region is intensively projected by O4 which is more an electronegative atom. The negative charge of the O13 atom is dominated by the positive charge of C6 atom resulting in poor red colour (yellow). The blue colour zone is influenced by all the hydrogen atoms, since all the hydrogen atoms have positive charge. The MBPA contains four oxygen atoms, which have more electron density holding capacity. It is obvious from Figure 5. That the region around oxygen atoms linked with carbon through double bond represents the most negative potential region (red). The hydrogen atoms attached to the ends of the methyl group possess the maximum positive charge. The predominance of the green region in the ring surfaces corresponds to a potential half way between the two extremes red and blue colour. Thus, the total electron density surface mapped with electrostatic potential clearly reveals the presence of high negative charge on the carbonyl oxygen (O4) in the COOH group, while more positive charge around two methylene groups and hydrogen atom in the COOH.



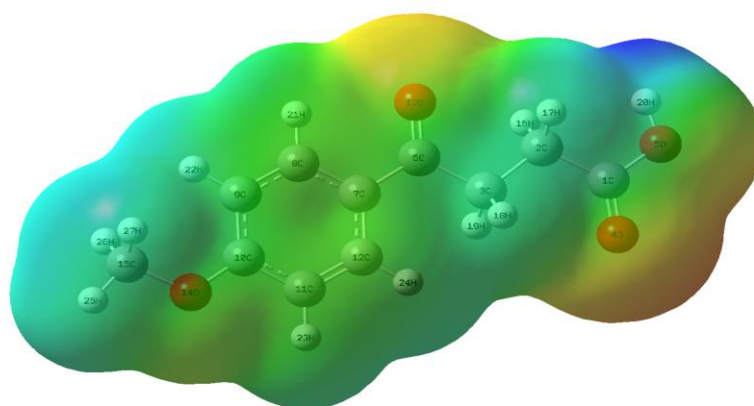


Fig 5. Molecular Electrostatic Potential (MESP) Of MBPA.

4.7. UV-Vis Studies

The UV-Vis Spectra Measured In Ethanol And Water Solution Are Shown In Fig 6. In This Work, On The Basis Of A Fully Optimized Ground State Structure, The Electronic Spectra Of MBPA Were Computed In Water And Ethanol Environment Using The TD-DFT Method At B3LYP/6-311++G(D,P) Level. The Experimental Absorption Spectrum Consists Of Three Peaks Around 199nm, 218nm And 270nm. All The Three Peaks Arise From The $\Pi - \Pi^*$ Transition Of The Benzene Ring As The Absorption Value Is So High. The Theoretical Spectrum Has The Λ_{\max} Value At 279nm With The Oscillator Strength 0.4843. This Corresponds From The Excitation Of HOMO To LUMO Transition. So The Experimental Result Completely Matches With The Calculated Absorption Spectrum.

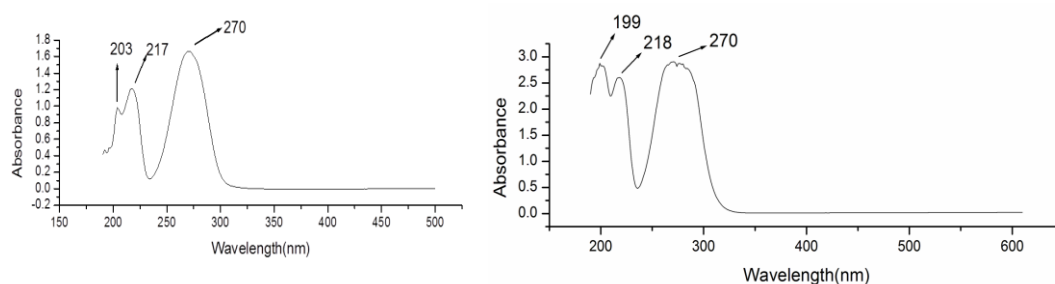


Fig 6 Experimental UV-Vis Spectra Of MBPA In Ethanol And Water Solvents.

V. Conclusion

The Structure Is Investigated By Utilizing Density Functional Theory Calculations With HF(6-31G) And B3LYP/6-31++G(D,P), B3LYP/6-311++G(D,P) Basis Sets. The Optimized Geometrical Parameters Obtained By B3LYP Method Show Good Agreement With The Experimental Data. The Vibrational Properties Of 3-(4-Methoxybenzoyl)Propionic Acid Have Been Investigated By FT-IR And FT-Raman Spectroscopies And Were Performed On The Basis Of B3LYP/6-31++G(D, P) And B3LYP/6-31++G(D, P) Methods. Vibrational Frequencies, Infrared Intensities And Raman Activities Calculated By B3LYP/6-311++G(D, P) Method Agree Very Well With The Experimental Result. NBO Study Explains The Charge Delocalization Of The Molecule. HOMO-LUMO Energy Gap Explains The Eventual Charge Transfer Interactions Taking Place Within The Molecule. The High Electronegativity Region In The O4 Atom Of COOH And The More Positive Region In The Methylene Groups Are Identified In The Molecular Electrostatic Potential Analysis. The Calculated UV-Vis Spectrum Using The TD-DFT Method Has The Absorption Maximum Peak At 279 Nm And It Matches With The Experimental Value.

References

- [1]. M.N. Haque, R. Chowdhury, K.M.S. Islamand, M.A. Akbar And Bang, J Anim Sci,98 (2009)115.
- [2]. Keshav, K.L. Wasewar, S. Chand And H. Uslu, Fluid Phase Equilibria, 21 (2009)275.
- [3]. www.Marketsandmarkets.Com
- [4]. www.Linkedin.Com
- [5]. En.Wikipedia.Org/Wiki/Ibuprofen
- [6]. M.J. Frisch Et Al., GAUSSIAN 03 Program, Gaussian, Inc.,Wattingford. CT. 2004.

- [7]. G. Rauhut And P. Pulay, J. Phys. Chem, 99 (1995)3093.
[8]. P. Pulay, G. Fogarasi, G. Pongoe, J.E. Boggs And A.J. Vargha Am Chem Soc, 105 (1983)7037.
[9]. G.Fogarasi, P.Pulay And J.R Durig(Eds.), Vibrational Spectra And Structure. Vol.14 Elsevier Publications. Amsterdam. 1985.
[10]. G. Fogarasi, N. Zhov, P.W. Taylor And P. Pulay, J Am Chem Soc, 114 (1992)8191.
[11]. T. Sundius, J Mol Struct, 218 (1990)321.
[12]. T. Sundius, Vib Spectrosc, 29 (2002)89.
[13]. G. Keresztury, S. Holly, J. Varga, G. Bensenyei, A.Y. Wang And J.R. Durig, Spectrochim Acta 49 (1993) 2007.
[14]. G. Keresztury, In : J.M. Chalmers And P.R. Griffith(Eds.), Raman Spectroscopy: Theory Hand Book Of Vibrational Spectroscopy, Vol. 1 John Wiley And Sons Ltd. New York, 2002, P. 71.
[15]. E.D. Glendening, A.E. Reed, J.E. Carpenter And F. Weinhold, NBO Version 3.1. TCI, University Of Wisconsin, Medison, 1998.
[16]. M. Kurt, M. Yurdakul And S. Kurdakul, J.Mol. Stuct.(Theochem)71 (2004)25.
[17]. H. Saleem, S. Subashchandrabose, Y. Erdogdu, V. Thanikachalam And J. Jayabharathi, Spectrochim.Acta A 101 (2013)91.
[18]. Yue Yang And Hongweigao, Spectrochim. Acta A 101 (2013)110.
[19]. G. Rauhut And P. Pulay, J. Phys. Chem, 99 (1995)3093.
[20]. F. Stuart, Infrared Spectroscopy; Fundamentals And Applications, John Wiley & Sons, Ltd., England. 2004.
[21]. G. Varsanyi, Vibrational Spectra Of Benzene Derivatives, Academic Press, New York, 1969.
[22]. D.I. Pavia, G.M. Lampman, G.S. Kriz And J. Vondeling(Eds.). Introduction To Spectroscopy, Third Edn., Thomson Learning, 2001, P. 579.
[23]. V. Krishnakumar, S. Dheivamalar, Spectrochim. Acta A 71 (2008)465.
[24]. N.P.G. Roeges, A Guide To Complete Interpretation Of The Infrared Spectra Of Organic Structures, Wiley, New York. 1954
[25]. Esmagunes, Cemalparlak, Spectrochim. Acta A 82 (2011)504.
[26]. N. Sundaraganesan, K. Sathesh Kumar, C. Meganathan And B. Dominic Joshua, Spectrochim Acta A 65 (2006)1186
[27]. N. Sundaraganesan, M. Priya, C. Meganathan, B. Dominic Joshua And J. Cornard, Spectrochim Acta A. 70 (2008)50.
[28]. J.M.S. Green, D.J. Harrison And W. Kynoston, Spectrochim.Acta A 27 (1971)807.
[29]. W.J. Balfour, Spectrochim. Acta A 39 (1983)780.
[30]. B. Venkatram Reddy And G. Ramanarao, Vib. Spectrosc, 6 (1994)231.
[31]. V. Ashokbabu, B. Lakshmaiah, K. Sreeramulu And G. Ramanarao, Ind J Pure & Appl Phys, 25 (1987)58.
[32]. B. Lakshmaiah And G. Ramanarao, J Raman Spectrosc, 20 (1989)439.
[33]. A.J. Abkowicz-Bienko, D.C. Bienko And Z. Latajka, J Mol Struct, 552 (2000)165.
[34]. V. Krishnakumar, S. Seshadri And S. Muthunatesan, Spectrochim. Acta A 68 (2007)811.
[35]. Jorly Joseph, E. D. Jemmis, J. Am. Chem. Soc. 129 (2007)4620.
[36]. N.B. Colthup, L.H. Daly And S.E. Wiberly, Introduction To Infrared Raman Spectroscopy, Academic Press, New York, 1990.
[37]. A.E. Ledesma, J. Zinczuk, A. Benaltabef, J.J. Lopez – Gonzalez And S.A. Brandan, J. Raman Spectroscopy Vol 40(8) (2009)1004.
[38]. S.A. Brandan, F. Marquez Lopez, M. Montejó, J.J. Lopez Gonzalez And A. Benaltabef, Spectrochim Acta Part A 75 (2010)1422.
[39]. Grabowski, J. Mol. Struct, 562 (2001)137.
[40]. W.J. Balfour, D. Risticpetrovic, J. Phys. Chem. 97 (1993)11643.
[41]. R.M. Silverstein And F.X. Webster, Spectrometric Identification Of Organic Compounds, Sixth Ed. John Wiley & Sons Inc., New York, 2003.
[42]. G. Kersztury, S. Holly, J. Varga, G. Besenyei, A.Y. Wang And J.R. Durig, Spectrochim. Acta A 49 (1993)2007.
[43]. D.L. Vein, N.B. Colthup, W.G. Fateley And J.G. Grasselli, The Handbook Of Infrared And Raman Characteristic Frequencies Of Organic Molecules, Academic Press, San Diego, 1991.
[44]. J. Choo, S. Kim, H. Joo And Y. Kwon, J Mol Struct (Theochem) 587(2002)1.
[45]. R.G. Pearson, Proc Natl Acad Sci 83 (1986)8440.

IOSR Journal of Applied Chemistry (IOSR-JAC) is UGC approved Journal with Sl. No. 4031, Journal no. 44190.

T.Chithambarathanu" Quantum Chemical Calculations on Vibrational and Electronic Structure Of 3-(4-Methoxybenzoyl) Propionic Acid" .IOSR Journal of Applied Chemistry (IOSR-JAC) 11.3 (2008):pp 42-53.